UNCLASSIFIED

AD 416695

DEFENSE DOCUMENTATION CENTER

FOR

SCIENTIFIC AND TECHNICAL INFORMATION

CAMERON STATION, ALEXANDRIA, VIRGINIA

UNCLASSIFIED

MASSACHUSETTS INSTITUTE OF TECHNOLOGY
DEPARTMENT OF NAVAL ARCHITECTURE AND MARINE ENGINEERING

LINEARIZED THEORY FOR PROPELLERS
IN STEADY FLOW

by

J. E. Kerwin

July, 1963

MASSACHUSETTS INSTITUTE OF TECHNOLOGY

Department of Naval Architecture and Marine Engineering

LINEARIZED THEORY FOR PROPELLERS
IN STEADY FLOW

by

J. E. Kerwin

July, 1963

Abstract

This report presents detailed derivations of the expressions for the steady-state disturbance velocity at a propeller blade due to pressure loading and thickness. A procedure for separating lifting line velocities from the total is outlined, and conclusions are drawn regarding the presence of camber and incidence corrections for propellers with symmetrical blades and chordwise load distributions.

i

Nomenclature

B = Kernel function for bound vortices defined in (5.9)

c = blade camber function

c_0 = maximum camber at a particular radius

D = vector distance defined in (5.2) and (6.2)

$f(v)$ = integrand of (6.8)

F_1, F_2 = functions defined in (A.2) and (A.3)

H_k = helicoidal surface representing k'th blade

i_a, i_t = axial and tangential induction factors defined in (A.5)

I = modified Bessel Function of the first kind

k = index identifying a particular blade

K = number of blades

K = modified Bessel Function of the second kind

ℓ = chord length of a blade section

n = normal coordinate in (s, r, n) system

P = pitch of a helicoidal surface

q = $\rho / \lambda(\rho)$

q_0 = $r / \lambda(\rho)$

r = radial coordinate in (x, r, θ) and (s, n, r) systems

r_h = radius of hub

$\vec{r}$ = unit vector in radial direction

R = propeller radius

s = streamwise coordinate in (s, n, r) system

s' = dummy streamwise coordinate

s_L, s_T = s coordinates of leading and trailing edge

11

$\vec{s}$ = unit vector in s direction

S = source kernel function defined in (3.11)

t = blade thickness function

t_o = maximum blade thickness at a particular radius

T = trailer kernel function defined in (6.9)

T_o = lifting-line part of T defined in (6.12)

T_1 = $T - T_o$

$\bar{u}, \bar{u}_a$ = x component of disturbance due to a unit singularity

$\bar{u}_t$ = tangential component of disturbance due to a unit singularity

$\bar{u}_r$ = radial component of disturbance due to a unit singularity

$\bar{u}_s$ = streamwise component of disturbance due to a unit singularity

$\bar{u}_n$ = normal component of disturbance due to a unit singularity

u_n = total disturbance velocity normal to blade

$u_n^{(s)}$ = normal velocity due to sources

$u_n^{(b)}$ = normal velocity due to bound vortices

$u_n^{(t)}$ = normal velocity due to trailers

$u_n^{(t_o)}$ = normal velocity due to lifting-line part of trailers T_o

$u_n^{(t_1)}$ = normal velocity due to T_1

U = function defined in (A.4)

$\bar{v}$ = y component of disturbance velocity due to a unit singularity

V_A = axial approach flow to propeller

V_o = relative flow past a blade section, neglecting disturbance velocities

V^* = relative flow past a blade section, including lifting-line disturbance velocities

$\bar{w}$ = z component of disturbance velocity due to a unit singularity

x = axial coordinate of (x, y, z) system--positive downstream

y = coordinate through tip of first blade in (x, y, z) system

z = third coordinate of (x, y, z) system

α = angle of incidence

β = advance angle--neglecting disturbance velocities

β_i = advance angle--including lifting-line disturbance velocities

γ = strength of bound vortex distribution-dimensions of velocity

γ_s = strength of trailing vortex sheet

Γ = radial circulation distribution--dimensions of velocity x length

δ_k = θ coordinate of tip of k'th blade

Δp = pressure difference between upper and lower surface of blade

ζ = dummy z coordinate

η = dummy y coordinate

θ = angular coordinate in (x, r, θ) system

θ_L, θ_T = angular coordinates of leading and trailing edge

λ = advance coefficient--neglecting disturbance velocities

λ_i = hydrodynamic advance coefficient

μ = $\varphi - \theta$

υ = $\varphi' - \theta$

ξ = dummy x coordinate

ξ' = dummy ξ' coordinate

ρ = dummy r coordinate

$\bar{\rho}$ = fluid mass density

σ = source strength per unit area-- dimensions of velocity

φ = dummy θ coordinate

φ' = dummy φ coordinate

Φ = velocity potential

ω = propeller rotational speed--radians per second

ρ' = dummy ρ coordinate

1. Introduction

A linearized theory for propellers can be developed as a logical extension of the theory of finite wings in incompressible flow. The principal difference is that a point on a propeller blade describes a helicoidal path as it moves through the fluid, while a point on a wing simply moves along a straight line. Although the general form of the expressions relating shape to pressure distribution is similar in both cases, the propeller expressions are naturally more complicated due to the more involved geometry of the motion.

We begin by stating the usual assumptions that the fluid is frictionless, incompressible, free of cavitation and infinite in extent. The propeller is considered to be operating in an axially directed stream whose magnitude is a function of radius only, and it is assumed that there are no extraneous solid boundaries. The flow is therefore steady relative to a coordinate system rotating with the propeller.

The propeller is assumed to have K symmetrically spaced identical blades. In the present work the existence of a propeller hub is neglected entirely. The propeller blades begin at some radius r_h which corresponds to the radius of the hub in the actual propeller. Both the inner and outer extremities of the blades are therefore regarded as free ends when the lift is required to be zero. This assumption is obviously not particularly realistic, and work is presently in progress to represent the hub properly as a solid cylindrical boundary. However, since the

1

inner part of the blade near the hub contributes only a small portion of the total propeller thrust, the "hubless propeller" approximation may be adequate.

In the linearized case we assume that the disturbance to the flow caused by the propeller is small, which requires that the blades be thin and that the camber and incidence of the blade sections relative to the undistrubed flow be small. As in linearized wing theory, the effects of thickness and of camber and incidence can be considered separately. Both can be represented by singularities distributed on stream surfaces formed by the undisturbed relative flow past the blades.

Blade thickness can be represented by a distribution of sources and sinks whose strength is proportional to the slope of the thickness form in the streamwise direction. Similarly, the discontinuity in pressure across the lifting surface can be generated by a distribution of vorticity whose axis is on the lifting surface and normal to the oncoming flow. These are designated "bound vortices." The condition of continuity of vorticity requires the presence of an additional distribution of vorticity whose axis is oriented in the direction of the relative flow. These vortices known as "trailers" are present not only on the blade surface but extend to infinity in the wake behind each blade.

There are obviously a large number of possible types of problems to which steady-state propeller theory may be applied. However, the following three are of principal interest:

1) Determine the shape of the blade sections for a prescribed radial and chordwise load distribution.

2) Determine the maximum camber and incidence of a given type of section at each radius in such a way that a prescribed radial load is achieved with the sections operating at their ideal angle of attack.

3) Determine the load distribution for a given shape.

2

The first problem is the most straight forward. We assume that the blade outline and thickness distribution have been determined from considerations of strength and cavitation. With both the load and thickness specified, the strengths of the sources, bound vortices and trailers are immediately known. The velocity normal to the blades at each point induced by each of these three singularity distributions may be determined by integration. The slope of the section mean line, according to the linear theory, is equal to the normal component of the disturbance velocity divided by the magnitude of the undisturbed approach flow. Consequently, if the normal component of the disturbance is known, the section shape can easily be determined by integration.

An important consideration is that the shape of the section mean lines required for a particular load depends not only on the load but also on the thickness of the blades. This is not true in the case of a planar lifting surface since the sources cannot induce a velocity normal to the plane on which they are situated. However, in the case of a propeller, the sources can induce a velocity normal to the blade on which they are situated as well as normal to the adjacent blades.

The second problem is somewhat more complicated since the chordwise load is initially unknown. However, as in the case of wing lifting surface theory, the chordwise load can be assumed to be composed of a finite number of modes whose form is determined from two-dimensional theory. The normal velocity induced by each mode can be determined in the same way as in the first problem. Since the total load at each chordwise section is prescribed, the amplitudes of some of the chordwise modes are known initially. The camber, incidence and amplitudes of the remaining modes can then be obtained by collocation.

3

The third case, which is sometimes call the "inverse problem," can be solved by assuming that the unknown load distribution is composed of a double summation of chordwise and radial modes. The normal velocity induced at a set of points by each mode can be determined as before and the unknown amplitudes obtained by collocation. This type of problem would arise if one wished to analyze the performance of a propeller operating at other than design conditions.

In the following sections, detailed derivations are given for the disturbance velocities due to the source and vortex systems representing the propeller. Much of this material may be found in recent publications by a number of authors. In particular, it should be mentioned that the results given here in section 4, 5, and 6 are in complete agreement with corresponding results given by Sparenberg [1] and by Pien [2], provided the proper conversion of nomenclature is made. Numerical techniques and results have not been included in this report but may be found in references [3] -- [7].

2. Geometrical Considerations

We begin by defining a Cartesian (x, y, z) coordinate system which is fixed on the propeller. As shown in Fig. 2.1, the x axis is the axis of revolution with positive distances measured downstream. The y axis is selected so as to pass through the tip of one blade, while the z axis completes the right-handed system. It is also convenient to define a cylindrical (x, r, θ) system where the x axis, as before, is the axis of revolution. The radial coordinate is denoted by r, and the angular coordinate (measured clockwise starting from the y axis) by θ. The equations relating the two systems are:

$$y = r \cos\theta \qquad\qquad r = \sqrt{y^2 + z^2}$$

$$z = r \sin\theta \qquad\qquad \theta = \tan^{-1}(z/y) \qquad\qquad (2.1)$$

In order to relate corresponding points on each of the K blades, we define δ_k as the θ coordinate of the point at the tip of the k'th blade. Assuming that the blades are symmetrically arranged, these angles are:

$$\delta_k = \frac{2\pi(k-1)}{K} \qquad\qquad k = 1, 2 \ldots K \qquad\qquad (2.2)$$

which is illustrated in Fig. 2.2.

In order to conserve symbols, we will assume at the outset that the propeller radius R is equal to unity. This is equivalent to saying that all length dimensions (including those present in linear velocities) have been divided by R.

The undisturbed flow past the blades is composed of a tangential component ωr due to the rotation of the propeller, and an
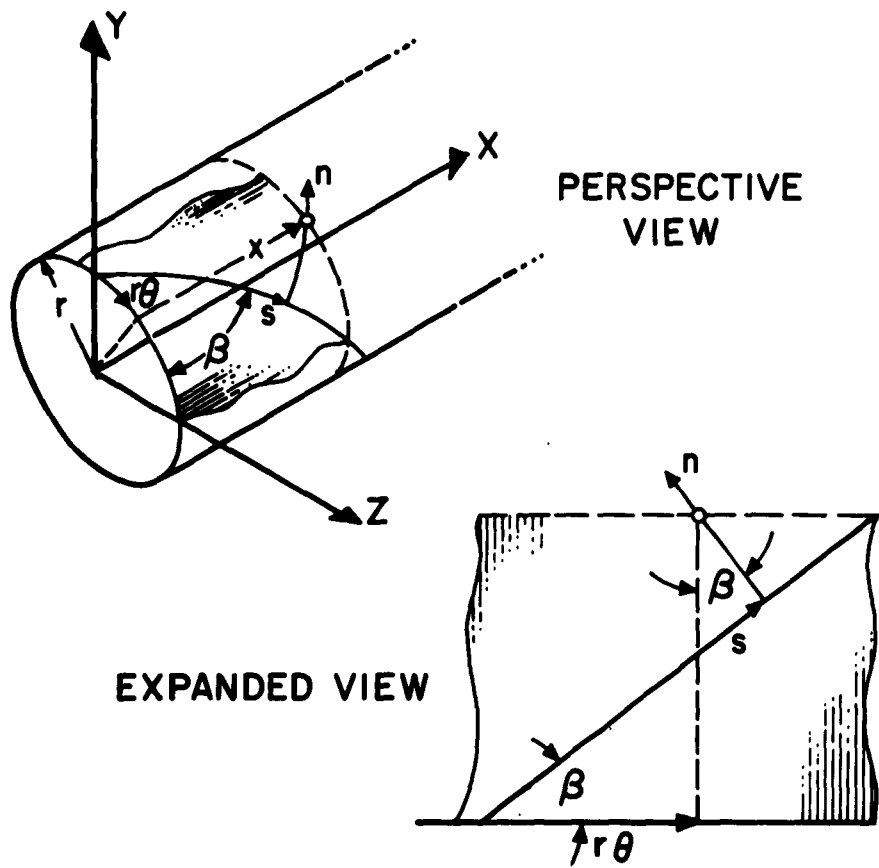
5
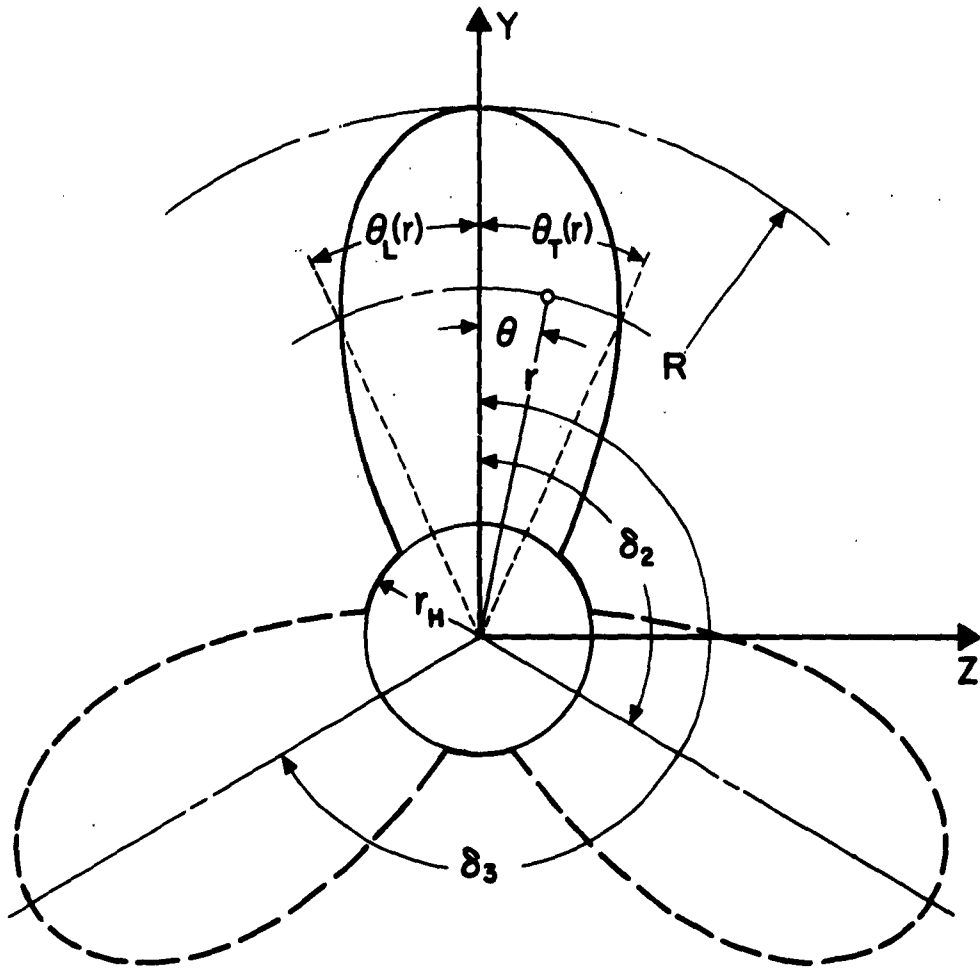
6

FIG.2.1 COORDINATE SYSTEMS

FIG. 2.2 PROJECTED BLADE OUTLINES

axial component $V_A(r)$ due to the oncoming stream. Since there is no radial component, the streamlines lie on cylindrical surfaces, r = constant. The angle between the undisturbed relative flow and the yz plane can be seen from Fig. 2.3 to be:

$$\beta(r) = \tan^{-1}\left(\frac{V_A(r)}{\omega r}\right) = \tan^{-1}\left(\frac{\lambda(r)}{r}\right) \tag{2.3}$$

where β is known as the advance angle and

$$\lambda(r) = r \tan\beta(r) \tag{2.4}$$

is defined as the advance coefficient. The streamlines are therefore helices whose pitch $P(r)$ is equal to $2\pi\lambda(r)$.

The sine and cosine of the advance angle, which will appear frequently in the following sections, can be expressed in terms of r and λ

$$\sin\beta(r) = \frac{\lambda(r)}{\sqrt{r^2 + \lambda^2(r)}}$$

$$\tag{2.5}$$

$$\cos\beta(r) = \frac{r}{\sqrt{r^2 + \lambda^2(r)}}$$

as can easily be seen from (2.3).

We next assume that the propeller blades lie approximately on the helicoidal surfaces swept out by the undisturbed flow past the radial lines

$$\left.\begin{array}{c} \theta = \delta_k \\ x = 0 \end{array}\right\} \tag{2.6}$$

This does not impose any restriction on the blade outline, but

8

neglects the effect of blade rake.

The k'th blade and its wake is therefore located approximately on the helicoidal surface

$$H_k(x, r, \theta) = x - \lambda(r)(\theta - \delta_k) = 0 \tag{2.7}$$

It is also convenient to define an orthogonal curvilinear coordinate system (s, n, r) on each of the H_k surfaces. The s coordinate is formed by the intersection of an axial cylinder and the surface H_k, and is therefore tangent to the streamlines of the undisturbed flow. The r coordinate is radial, as before, and the n coordinate is perpendicular to r and s is directed in such a way that it has a positive axial component. This notation is illustrated in Fig. 2.1.

If the pitch of the helicoidal surface is independent of radius, the r coordinate through any point on $\dot{H}_k$ remains on H_k. The n coordinate is therefore normal to H_k. If the pitch is a function of radius, this is not necessarily true so that n may depart slightly from the true normal to the helicoidal surface. However, it is assumed that variations in pitch are sufficiently gradual for this discrepancy to be negligible.

As can be seen from Fig. 2.1, the expressions relating the (s, n, r) and (x, r, θ) coordinate systems are:

$$s = x \sin\beta + r(\theta - \delta_k) \cos\beta = \frac{\lambda(r) x + r^2(\theta - \delta_k)}{\sqrt{r^2 + \lambda^2(r)}}$$

$$n = x \cos\beta - r(\theta - \delta_k) \sin\beta = \frac{xr - r\lambda(\theta - \delta_k)}{\sqrt{r^2 + \lambda^2(r)}} \tag{2.8}$$

10

On any one of the K helicoidal surfaces, the relationship between x and θ can be obtained by combining (2.7) and (2.8)

$$s = \sqrt{r^2 + \lambda^2(r)} \; (\theta - \delta_k) \qquad (2.9)$$

We can now define the blade outline and the shape of the blade sections in the (s, n, r) system. The s coordinates of the leading and trailing edges are $s_L(r)$ and $s_T(r)$ respectively, while the angular coordinates are designated $\theta_L(r)$ and $\theta_T(r)$.

$$\ell(r) = s_T(r) - s_L(r) \qquad (2.10)$$

The blade sections can be decomposed (as in two-dimensional wing theory) into a symmetrical thickness form $t(s, r)$, a mean line $c(s, r)$ and an angle of incidence $\alpha(r)$. The maximum thickness of a section at a particular radius is denoted $t_o(r)$ and the maximum camber is $c_o(r)$. This notation is shown in Fig. 2.4.
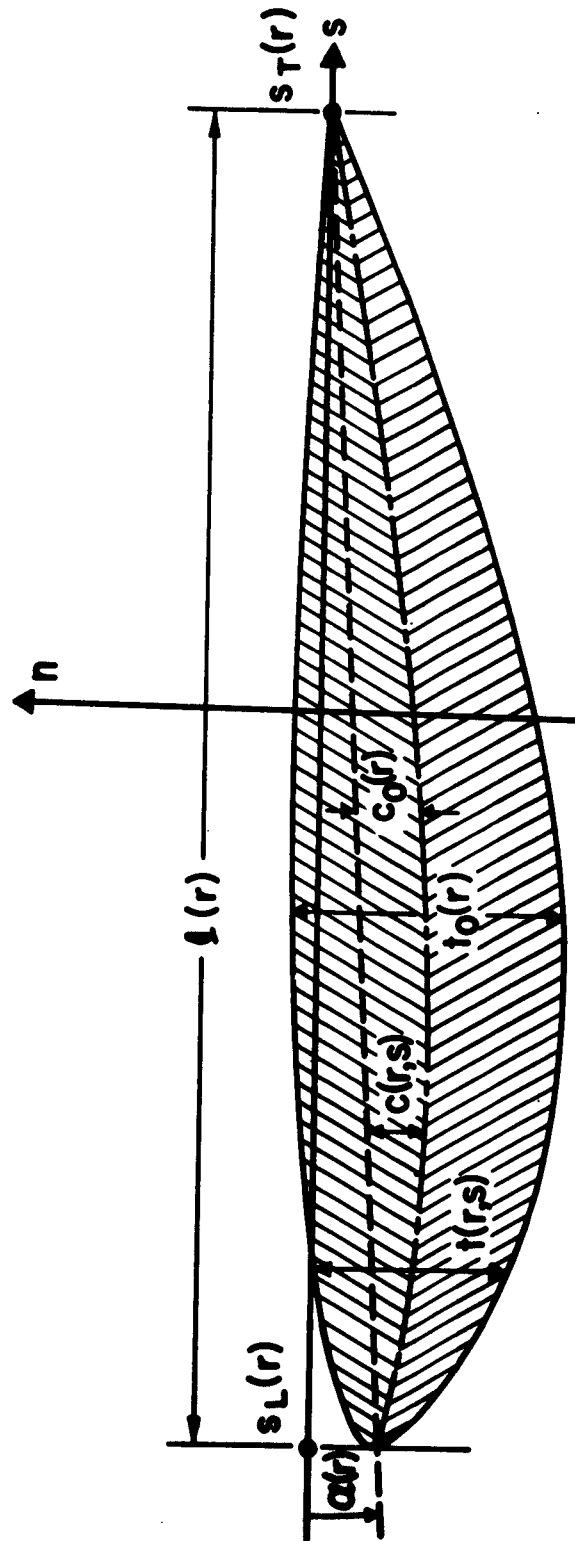
FIG. 2.4 ILLUSTRATION OF BLADE SECTION NOTATION

3. Normal Velocity Induced by Blade Thickness

According to linear theory, the thickness of the blades can be generated by a distribution of sources and sinks located on the helicoidal surfaces representing the blades. We consider first a point source of unit strength located at a point with Cartesian coordinates (ξ, η, ζ). The velocity potential if this source is

$$\Phi(x, y, z) = \frac{-1}{4\pi\sqrt{(x - \xi)^2 + (y - \eta)^2 + (z - \zeta)^2}} \qquad (3.1)$$

and the Cartesian components of velocity at (x, y, z) are

$$\bar{u}(x, y, z, \xi, \eta, \zeta) = \frac{\partial \Phi}{\partial x} = \frac{x - \xi}{4\pi\left[(x - \xi)^2 + (y - \eta)^2 + (z - \zeta)^2\right]^{3/2}}$$

$$(3.2)$$

$$\bar{v}(x, y, z, \xi, \eta, \zeta) = \frac{\partial \Phi}{\partial y} = \frac{y - \eta}{4\pi\left[(x - \xi)^2 + (y - \eta)^2 + (z - \zeta)^2\right]^{3/2}}$$

$$\bar{w}(x, y, z, \xi, \eta, \zeta) = \frac{\partial \Phi}{\partial z} = \frac{z - \zeta}{4\pi\left[(x - \xi)^2 + (y - \eta)^2 + (z - \zeta)^2\right]^{3/2}}$$

The bars on the symbols (u, v, w) denote velocities due to a point source of unit strength. The total velocity at a point due to a distribution of sources is identified by the same symbol but without

13

a bar on top. It should be mentioned that the symbols (u, v, w) will not be used exclusively for source velocities but will be used to denote disturbance velocity components in general. Since we are considering only sources in this section, there is no need for further identification. However, additional symbols will have to be introduced later to distinguish between disturbance velocities due to source and vortex distributions.

The velocity components given in (3.2) can be converted to cylindrical coordinates using the equivalent of (2.1)

$$y = r \cos\theta \qquad z = r \sin\theta$$
$$\eta = \rho \cos\varphi \qquad \zeta = \rho \sin\varphi \tag{3.3}$$

where (x, r, θ) is the point where the velocity is to be evaluated and (ζ, ρ, φ) is the location of the source. The axial tangential and radial components are

$$\bar{u}_a(x,r,\theta,\zeta,\rho,\varphi) = \frac{x - \zeta}{4\pi\left[(x - \zeta)^2 + r^2 + \rho^2 - 2r\rho \cos(\varphi - \theta)\right]^{3/2}}$$

$$\bar{u}_t(x,r,\theta,\zeta,\rho,\varphi) = \bar{w} \cos\theta - \bar{v} \sin\theta = \frac{-\rho \sin(\varphi - \theta)}{4\pi\left[(x - \zeta)^2 + r^2 + \rho^2 - 2r\rho \cos(\varphi-\theta)\right]^{3/2}}$$

$$\bar{u}_r(x,r,\theta,\zeta,\rho,\varphi) = \bar{w} \sin\theta + \bar{v} \cos\theta = \frac{r - \rho \cos(\varphi - \theta)}{4\pi\left[(x - \zeta)^2 + r^2 + \rho^2 - 2r\rho\cos(\varphi-\theta)\right]^{3/2}}$$

14

The velocity components given in (3.4) can be resolved into components in the helicoidal coordinate system by means of (2.8)

$$\bar{u}_s(x, \ r, \ \theta, \ \xi, \ \rho, \ \varphi) = \frac{\lambda(r)\bar{u}_a + r\bar{u}_t}{\sqrt{r^2 + \lambda^2(r)}}$$

$$\bar{u}_n(x, \ r, \ \theta, \ \xi, \ \rho, \ \varphi) = \frac{r\bar{u}_a - \lambda(r)\bar{u}_t}{\sqrt{r^2 + \lambda^2(r)}}$$

(3.5)

In this application, we are only interested in the velocity normal to the helicoidal surface. This can be obtained by combining (3.4) and (3.5)

$$\bar{u}_n(x, \ r, \ \theta, \ \xi, \ \rho, \ \varphi) = \frac{r(x - \xi) + \lambda(r)\rho \, \sin(\varphi - \theta)}{4\pi\sqrt{r^2 + \lambda^2(r)}\left[(x - \xi)^2 + r^2 + \rho^2 - 2r\rho \, \cos(\varphi-\theta)\right]^{3/2}}$$

(3.6)

For points on the helicoidal surfaces representing the blades, x and ξ are related to θ and φ by (2.7). If we adopt the point of view that the velocity is always to be computed at a point (x, r, θ) on the first blade, while the position of the source is at some point (ξ, ρ, $\varphi + \delta_k$) on the k'th blade, there follows

$$x = \lambda(r)\theta$$
$$\xi = \lambda(\rho)\varphi$$

(3.7)

so that (3.6) becomes

$$\bar{u}_h(r, \theta, \rho, \varphi, k) = \frac{r(\lambda(r)\theta - \lambda(\rho)\varphi) + \lambda(r)\rho \sin(\varphi + \delta_k - \theta)}{4\pi\sqrt{r^2 + \lambda^2(r)}\left[(\lambda(r)\theta - \lambda(\rho)\varphi)^2 + r^2 + \rho^2 - 2r\rho\cos(\varphi + \delta_k - \theta)\right]^{3/2}}$$

$$(3.8)$$

If λ is independent of radius, the term $(\lambda(r)\theta - \lambda(\rho)\varphi)$ appearing both in the numerator and denominator of (3.8) can be replaced by $\lambda(\theta - \varphi)$. In this case, the angles φ and θ in (3.8) appear only in the combination $(\varphi - \theta)$, which is equivalent to saying that the velocity depends only on the angle between the source and the point. Since this represents a great simplification, it is worthwhile in the general case to introduce the approximation

$$\lambda(r)\theta - \lambda(\rho)\varphi \approx -\lambda(\rho)(\varphi - \theta) = -\lambda(\rho)\mu \qquad (3.9)$$

where, by definition

$$\mu = \varphi - \theta \qquad (3.10)$$

The geometrical interpretation of this approximation is that the axial distance between the point at (x, r, θ) and the singularity at (ξ, ρ, φ) is assumed to be the same as if the pitch of the helicoidal surface at ρ were the same as at r. If the variation of λ with r is gradual, the error in axial distance will be small when ρ is close to r. Consequently, the error introduced in determining the velocity induced by nearby source elements would presumably be small. For distant elements, on the other hand, a change in the axial component of the distance between two elements will not have a large effect on the direction or magnitude of the induced velocity.

Of course, when λ is constant, there is no approximation involved.

Substituting (3.9) into (3.8) and summing over the K blades, we obtain the result

$$S(r,\rho,\mu) = \frac{\lambda(\rho)}{4\pi\sqrt{r^2+\lambda^2(r)}} \sum_{k=1}^{K} \frac{-r\mu + \rho \sin(\mu + \delta_k)}{\left[\lambda^2(\rho)\mu^2+ r^2 + \rho^2 - 2r\rho \cos(\mu + \delta_k)\right]^{3/2}}$$

(3.11)

where $S(r,\rho,\mu)$ represents the velocity normal to the helicoidal surface at a point (r, θ) on the first blade induced by K unit point sources at a radius ρ. The angular coordinates of the sources are $(\varphi + \delta_k - \theta)$ measured from the y axis, or $(\mu + \delta_k)$ measured from the point (r, θ). It can be seen from (3.11) that $S(r,\rho,\mu)$ is an odd function of μ,

$$S(r,\rho,-\mu) = -S(r,\rho,\mu)$$

(3.12)

This is obviously true when $k = 1$. When $k > 1$, the contribution of the k'th blade to S is odd provided that we change the sign of δ_k as well as μ. Since the sign change is equivalent to summing the blades in the reverse order, the total result is unaffected, hence we conclude that S is odd.

We next need to determine the strength of the source distribution. According to linear theory, the source strength per unit area, σ, is given by[8]

$$\sigma(\rho, \varphi) = V_o(\rho) \frac{\partial t}{\partial s} (\rho, \varphi)$$

(3.13)

17

where V_o is the magnitude of the undisturbed relative flow and $\frac{\partial t}{\partial s}$ is the derivative of the thickness form in the streamwise direction. It is evident from Fig. 2.3 that

$$V_o(\rho) = \frac{V_A(\rho)}{\sin\beta(\rho)} = \frac{V_A(\rho)\sqrt{\rho^2 + \lambda^2(\rho)}}{\lambda(\rho)} \qquad (3.14)$$

so that

$$\sigma(\rho,\varphi) = \frac{V_A(\rho)\sqrt{\rho^2 + \lambda^2(\rho)}\ \frac{\partial t}{\partial s}(\rho,\varphi)}{\lambda(\rho)} \qquad (3.15)$$

The total normal velocity at any point on the first blade can now be obtained by combining (3.11) and (3.15) and integrating over the surface of the first blade

$$u_n^{(s)}(r,\theta) = \int_{\rho=r_h}^{1.0} \int_{s=s_L(\rho)}^{s_T(\rho)} \sigma(\rho,\varphi)\ S(r,\ \rho,\ \mu)\ ds\ d\rho \qquad (3.16)$$

The chordwise integration in (3.16) can be expressed entirely in terms of the variable μ by introducing

$$ds = \sqrt{\rho^2 + \lambda^2(\rho)}\ d\mu$$

$$\varphi = \mu + \theta \qquad (3.17)$$

18

so that

$$u_n^{(s)}(r,\theta) = \int_{\rho=r_h}^{1.0} \int_{\mu=\theta_L-\theta}^{\theta_T-\theta} \sigma(\rho,\mu+\theta)\, S(r,\rho,\mu)\, \sqrt{\rho^2+\lambda^2(\rho)}\,d\mu\, d\rho \qquad (3.18)$$

While the integration in (3.18) cannot be carried out explicitly in most cases, various numerical schemes are available which will yield results of sufficient accuracy. It is important to note that the integral in this case is not singular since $S(r,\rho,\mu)$ has a finite limit when $r\to\rho$ and $\mu\to0$.

4. Distribution of Bound Vortices and Trailers

The pressure loading on the blades can be represented by a distribution of radially oriented bound vortices lying on the helicoidal surfaces representing the blades. We again introduce the dummy cylindrical coordinates $(\varsigma, \rho, \varphi)$ to denote the location of an element of the vortex sheet, while (x, r, θ) are the coordinates of a point at which the velocity is to be determined. The strength of the bound vortex sheet per unit of length along the helix at radius ρ is $\gamma(\rho, \varphi)$. The pressure difference across the surface according to linear theory is[8]

$$\Delta p (\rho, \varphi) = \bar{\rho} \, V_o(\rho) \, \gamma(\rho, \varphi) \tag{4.1}$$

where $\bar{\rho}$ is the fluid density. Substituting (3.14) for the approach velocity V_o in (4.1) there follows

$$\Delta p(\rho, \varphi) = \frac{\overline{\rho} V_A(\rho) \sqrt{\rho^2 + \lambda^2(\rho)} \; \gamma(\rho, \varphi)}{\lambda(\rho)} \tag{4.2}$$

The total circulation around a blade at radius ρ is

$$\Gamma(\rho) = \int_{s_L(\rho)}^{s_T(\rho)} \gamma(\rho, \varphi) ds = \int_{\theta_L(\rho)}^{\theta_T(\rho)} \gamma(\rho, \varphi) \sqrt{\rho^2 + \lambda^2(\rho)} \, d\varphi \tag{4.3}$$

where θ_L and θ_T are the angular coordinates of the leading and trailing edges, respectively, and the element of arc length ds has been

expressed in terms of $d\varphi$ using (2.9).

In order to preserve continuity of vorticity, there must also be a system of trailing vortices whose axis is in the s direction. The requirement of continuity of vorticity on a helicoidal surface can be obtained very easily by keeping track of the total vorticity entering a differential element of the surface, as shown in Fig. 4.1. The strength of the vortex lines entering the four sides of the element is

$$
\text{bound circulation entering bottom} = \gamma(\rho,\varphi)\sqrt{\rho^2 + \lambda^2(\rho)}d\varphi
$$

$$
\text{bound circulation entering top} = -\gamma(\rho+d\rho,\varphi)\sqrt{(\rho+d\rho)^2 + \lambda^2(\rho+d\rho)}d\varphi
$$

$$
\text{trailers entering left} = \gamma_s(\rho,\varphi)\,d\rho
$$

$$
\text{trailers entering right} = -\gamma_s(\rho,\varphi + d\varphi)\,d\rho
$$

(4.4)

Setting the sum equal to zero gives the result

$$
\frac{\partial \gamma_s(\rho,\varphi)}{\partial\varphi} = -\frac{\partial}{\partial\rho}\left[\gamma(\rho,\varphi)\sqrt{\rho^2 + \lambda^2(\rho)}\right] \qquad (4.5)
$$

where γ_s denotes the strength of the trailer.

Equation (4.4) holds only for points in the interior of the blades. At the leading and trailing edges, a trailer is generated, so to speak, whenever a bound vortex tries to run off the edge. This can be seen by taking as the control area an infinitesimal triangular element as shown in Fig. 4.2. In order for the blade edge to form the hypotenuse of the triangular element, the relationship between $d\varphi$ and $d\rho$ must be

$$
\partial\varphi = \frac{\partial\theta_L}{\partial\rho}\,d\rho \qquad \text{at the leading edge.}
$$

(4.6)

$$
\partial\varphi = \frac{-\partial\theta_T}{\partial\rho}\,d\rho \qquad \text{at the trailing edge}
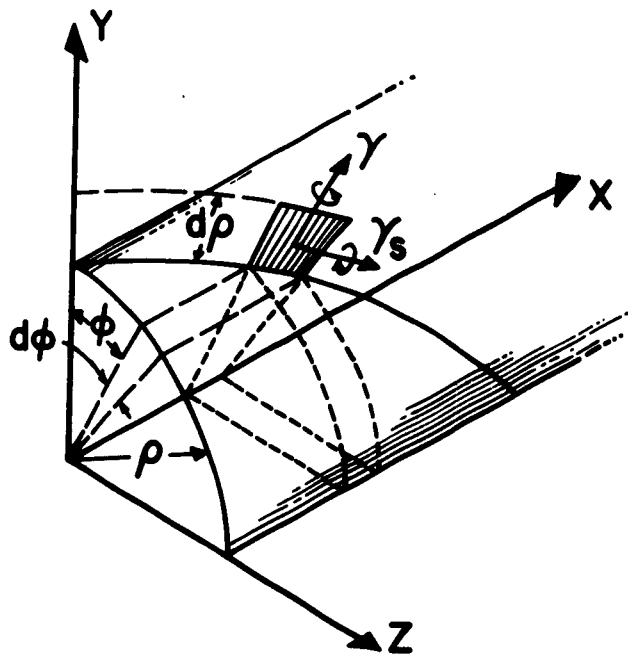$$

21

FIG. 4.1   ELEMENT OF VORTEX SHEET
IN INTERIOR OF BLADE

At the leading edge, the bound circulation entering the bottom as before is

$$\gamma(\rho, \theta_L) \sqrt{\rho^2 + \lambda^2(\rho)} \, d\varphi \tag{4.7}$$

while in this case, there is none leaving the top. This must be balanced by the total strength of the trailers entering the right side, which to a first order is

$$-\gamma_s(\rho, \theta_L) \, d\rho \tag{4.8}$$

Combining this with (4.6) and (4.7) gives the result

$$\gamma_s(\rho, \theta_L) = \gamma(\rho, \theta_L) \sqrt{\rho^2 + \lambda^2(\rho)} \; \frac{\partial \theta_L}{\partial \rho} \tag{4.9}$$

A similar analysis of circulation entering a triangular element at the trailing edge shows that γ_s must also be discontinuous at that point. If $\gamma_s(\rho, \theta_T^-)$ is the strength of the trailer just inside the trailing edge, and $\gamma_s(\rho, \theta_T^+)$ is the strength just outside the trailing edge, the following expressions hold to a first order

bound circulation entering bottom = $\gamma(\rho, \theta_T) \sqrt{\rho^2 + \lambda^2(\rho)} \, d\varphi$

bound circulation leaving top = 0

trailers entering left = $\gamma_s(\rho, \theta_T^-) \, d\rho$

trailers entering right = $-\gamma_s(\rho, \theta_T^+) \, d\rho$
$$\tag{4.10}$$

Setting the total equal to zero and introducing (4.6), there follows

$$\gamma_s(\rho, \theta_T^+) - \gamma_s(\rho, \theta_T^-) = -\gamma(\rho, \theta_T) \sqrt{\rho^2 + \lambda^2(\rho)} \; \frac{\partial \theta_T}{\partial \rho} \tag{4.11}$$

23
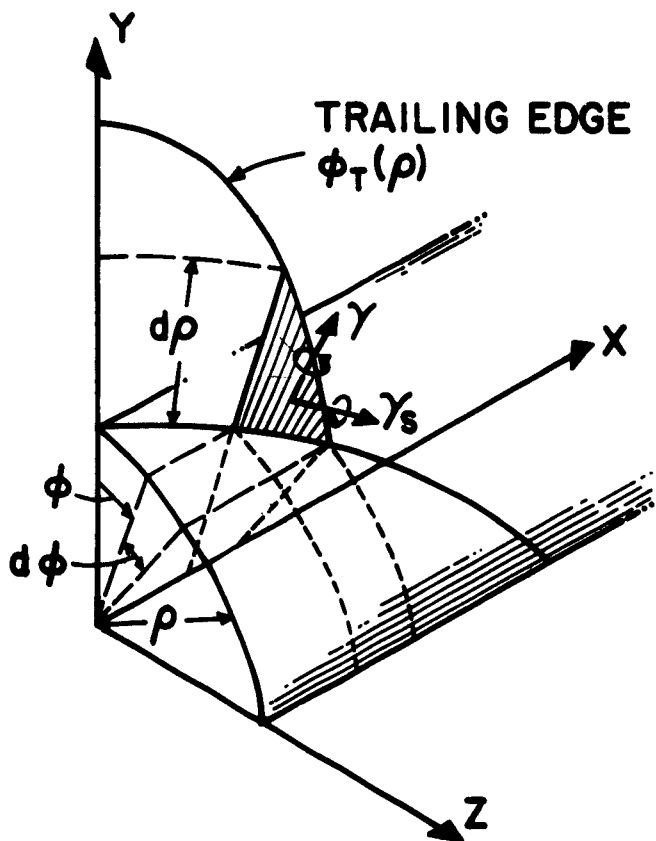
FIG. 4.2   ELEMENT OF VORTEX SHEET
              AT TRAILING EDGE

The total strength of the trailers at any point is obtained by integrating (4.5) and adding the contributions of the edges from (4.9) and (4.11)

$$\gamma_s(\rho,\varphi) = \gamma(\rho,\theta_L)\sqrt{\rho^2 + \lambda^2(\rho)}\ \frac{\partial\theta_L}{\partial\rho} - \int_{\theta_L(\rho)}^{\varphi} \frac{\partial}{\partial\rho}\left[\gamma(\rho,\varphi)\sqrt{\rho^2 + \lambda^2(\rho)}\right] d\varphi \qquad (4.$$

$$\text{for } \theta_L \leq \varphi < \theta_T$$

$$\gamma_s(\rho,\varphi) = \gamma(\rho,\theta_L)\sqrt{\rho^2 + \lambda^2(\rho)}\ \frac{\partial\theta_L}{\partial\rho} - \int_{\theta_L(\rho)}^{\theta_T(\rho)} \frac{\partial}{\partial\rho}\left[\gamma(\rho,\varphi)\sqrt{\rho^2 + \lambda^2(\rho)}\right] d\varphi$$

$$(4.$$

$$-\gamma(\rho,\theta_T)\sqrt{\rho^2 + \lambda^2(\rho)}\ \frac{\partial\theta_T}{\partial\rho}$$

$$\text{for } \theta_T \leq \varphi$$

Noting that the limits of integration above are functions of ρ, it is evident that (4.13) is equivalent to

$$\gamma_s(\rho,\varphi) = -\frac{\partial}{\partial\rho} \int_{\theta_L(\rho)}^{\theta_T(\rho)} \gamma(\rho,\varphi)\sqrt{\rho^2 + \lambda^2(\rho)}\ d\varphi = -\frac{\partial\Gamma(\rho)}{\partial\rho} \qquad (4.14)$$

$$\text{for } \theta_T \leq \varphi$$

25

5. Normal Velocity Induced by Bound Vortices

We determine next the velocity induced at a point (x, r, θ) by a bound vortex of unit strength located at a point (ξ, ρ, φ). Since there is no such thing as a "point vortex," what we will determine is the velocity induced per unit length of the vortex. This can be determined from the law of Biot-Savart, which in this case can be written:

$$(\bar{u}, \bar{v}, \bar{w}) = \frac{\vec{r} \times \vec{D}}{4\pi |D|^3} \tag{5.1}$$

where $\vec{r}$ is a unit vector in the radial direction, $\vec{D}$ is a vector from the vortex (ξ, ρ, φ) to the point (x, r, θ), and $(\bar{u}, \bar{v}, \bar{w})$ are the Cartesian components of velocity. The components of $\vec{D}$ can be seen from Fig. 5.1 to be:

$$\vec{D} = \left[(x - \xi),\ r \cos\theta - \rho \cos\varphi,\ r \sin\theta - \rho \sin \varphi \right] \tag{5.2}$$

while the components of a unit vector in the radial direction are

$$\vec{r} = \left[0,\ \cos\varphi,\ \sin\varphi \right] \tag{5.3}$$

Substituting (5.2) and (5.3) in (5.1) yields the following expression for the velocity components

$$\bar{u} = \frac{- r \sin(\varphi - \theta)}{4\pi \left[(x - \xi)^2 + r^2 + \rho^2 - 2r\rho\cos(\varphi - \theta) \right]^{3/2}}$$
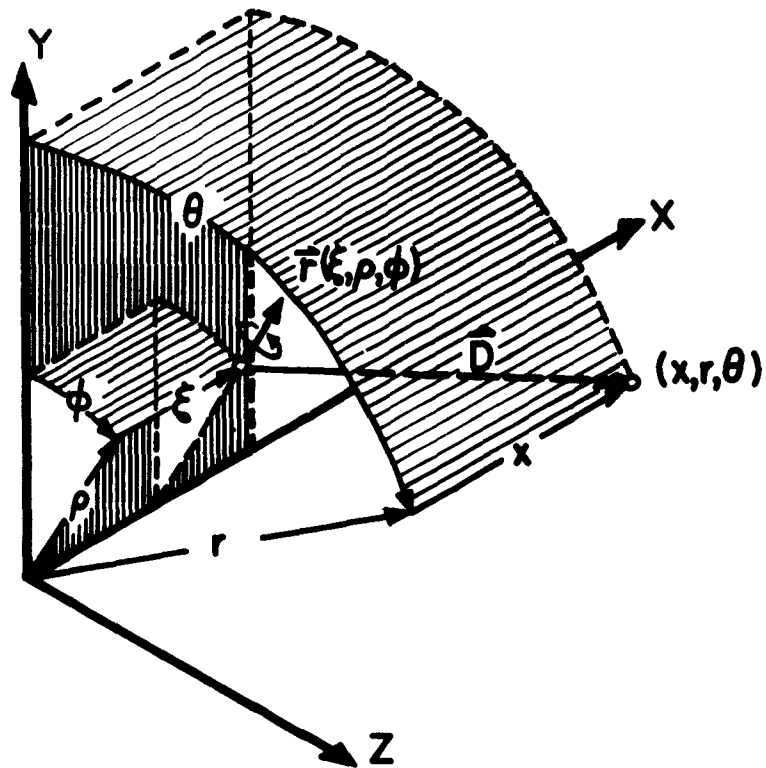
26

FIG. 5.1 NOTATION FOR VELOCITY AT (x, r, θ) INDUCED BY A BOUND VORTEX AT (ξ, ρ, ϕ)

$$\bar{v} = \frac{(x - \xi)\sin\varphi}{4\pi\left[(x - \xi)^2 + r^2 + \rho^2 - 2r\rho\cos(\varphi - \theta)\right]^{3/2}}$$

$$\bar{w} = \frac{-(x - \xi)\cos\varphi}{4\pi\left[(x - \xi)^2 + r^2 + \rho^2 - 2r\rho\cos(\varphi - \theta)\right]^{3/2}}$$

(5.4)

Proceeding in the same way as with the source expressions, we next convert to cylindrical coordinates using (3.3)

$$\bar{u}_a = \bar{u} = \frac{-r\sin(\varphi - \theta)}{4\pi\left[(x - \xi)^2 + r^2 + \rho^2 - 2r\rho\cos(\varphi - \theta)\right]^{3/2}}$$

(5.5)

$$\bar{u}_t = \bar{w}\cos\theta - \bar{v}\sin\theta = \frac{-(x - \xi)\cos(\varphi - \theta)}{4\pi\left[(x - \xi)^2 + r^2 + \rho^2 - 2r\rho\cos(\varphi - \theta)\right]^{3/2}}$$

$$\bar{u}_r = \bar{w}\sin\theta + \bar{v}\cos\theta = \frac{(x - \xi)\sin(\varphi - \theta)}{4\pi\left[(x - \xi)^2 + r^2 + \rho^2 - 2r\rho\cos(\varphi - \theta)\right]^{3/2}}$$

The component normal to the helicoidal surface is obtained by substituting (5.5) into (3.5)

$$\bar{u}_n(x,r,\theta,\xi,\rho,\varphi) = \frac{-r^2\sin(\varphi - \theta) + \lambda(r)(x - \xi)\cos(\varphi - \theta)}{4\pi\sqrt{r^2 + \lambda^2(r)}\left[(x - \xi)^2 + r^2 + \rho^2 - 2r\rho\cos(\varphi - \theta)\right]^{3/2}}$$

28

Equation (5.6) expresses the velocity induced at (x, r, θ) by a unit bound vortex at (ξ, ρ, φ). If we again consider the special case of the velocity induced at (r, θ) on the first blade by a unit bound vortex at $(\rho, \varphi + \delta_k)$ on the k'th blade, (5.6) becomes

$$(5.7)$$

$$\bar{u}_n(r,\theta,\rho,\varphi,k) = \frac{-r^2 \sin(\varphi-\theta+\delta_k) - \lambda(r)\left[\lambda(\rho)\varphi - \lambda(r)\theta\right]\cos(\varphi-\theta+\delta_k)}{4\pi\sqrt{r^2 + \lambda^2(r)} \left[(\lambda(\rho)\varphi - \lambda(r)\theta)^2 + r^2 + \rho^2 - 2r\rho\cos(\varphi-\theta+\delta_k)\right]^{3/2}}$$

where x and ξ have been eliminated using (3.7).

Introducing the approximation

$$\lambda(r)\theta - \lambda(\rho)\varphi \approx -\lambda(\rho)(\varphi - \theta) = -\lambda(\rho)\mu \qquad (5.8)$$

as before and summing over the K blades, we obtain the result

$$B(r,\rho,\mu) = \frac{1}{4\pi\sqrt{r^2 + \lambda^2(r)}} \sum_{k=1}^{K} \frac{-r^2 \sin(\mu + \delta_k) - \lambda(r)\lambda(\rho)\mu\cos(\mu + \delta_k)}{\left[\lambda^2(\rho)\mu^2 + r^2 + \rho^2 - 2r\rho\cos(\mu + \delta_k)\right]^{3/2}} \qquad (5.9)$$

In equation (5.9), $B(r, \rho, \mu)$ represents the normal velocity induced by K unit bound vortices and is analogous to the expression for the velocity induced by the unit sources given in (3.11). It is also evident that B is an odd function of μ provided that the blades are symmetrically arranged.

The total velocity at (r, θ) induced by a distribution of bound vortices can now be written as an integral over the surface of the first blade.

29

$$\prime u_n^{(b)}(r,\theta) = \int_{\rho=r_H}^{1.0} \int_{s=s_L(\rho)}^{s_T(\rho)} \gamma(\rho,\varphi)\, B(r,\rho,\mu)\, ds\, d\rho$$

(5.10)

$$= \int_{\rho=r_H}^{1.0} \int_{\mu=\theta_L-\theta}^{\theta_T-\theta} \gamma(\rho,\mu+\theta)\, B(r,\rho,\mu)\sqrt{\rho^2 + \lambda^2(\rho)}\, d\mu\, d\rho$$

In this case the integral is singular at the point $(\rho = r, \mu = 0)$ so that the Cauchy principal value must be taken.

6. Normal Velocity Induced by Trailers

We begin by determining the velocity induced at (x, r, θ) by a trailer of unit strength originating at a point (ξ, ρ, φ) and extending to infinity downstream. In order to distinguish a general point on the trailer from its starting point, the former is identified by the dummy coordinates (ξ', ρ', φ'). Since the radius of the trailer is assumed to be constant, the prime on ρ is unnecessary and will therefore be omitted.

The velocity can be expressed according to Biot-Savart's law and an integral along the vortex

$$(\bar{u}, \bar{v}, \bar{w}) = \frac{1}{4\pi} \int \frac{\vec{s} \times \vec{D}}{|D|^3} \, ds' \tag{6.1}$$

where $\vec{s}$ is a unit vector tangent to the trailer and ds' is a differential element of arc length along the trailer. Referring to Fig. 6.1, the vector from a general point $(\xi; \rho; \varphi')$ on the trailer to the point (x, r, θ) can be seen to be

$$\vec{D} = \left[(x - \xi'), \; r\cos\theta - \rho\cos\varphi', \; r\sin\theta - \rho\sin\phi' \right] \tag{6.2}$$

which is the same as (5.2) except for the primes on ξ' and φ'. A unit vector tangent to a helix with an advance coefficient $\lambda(\rho)$ is

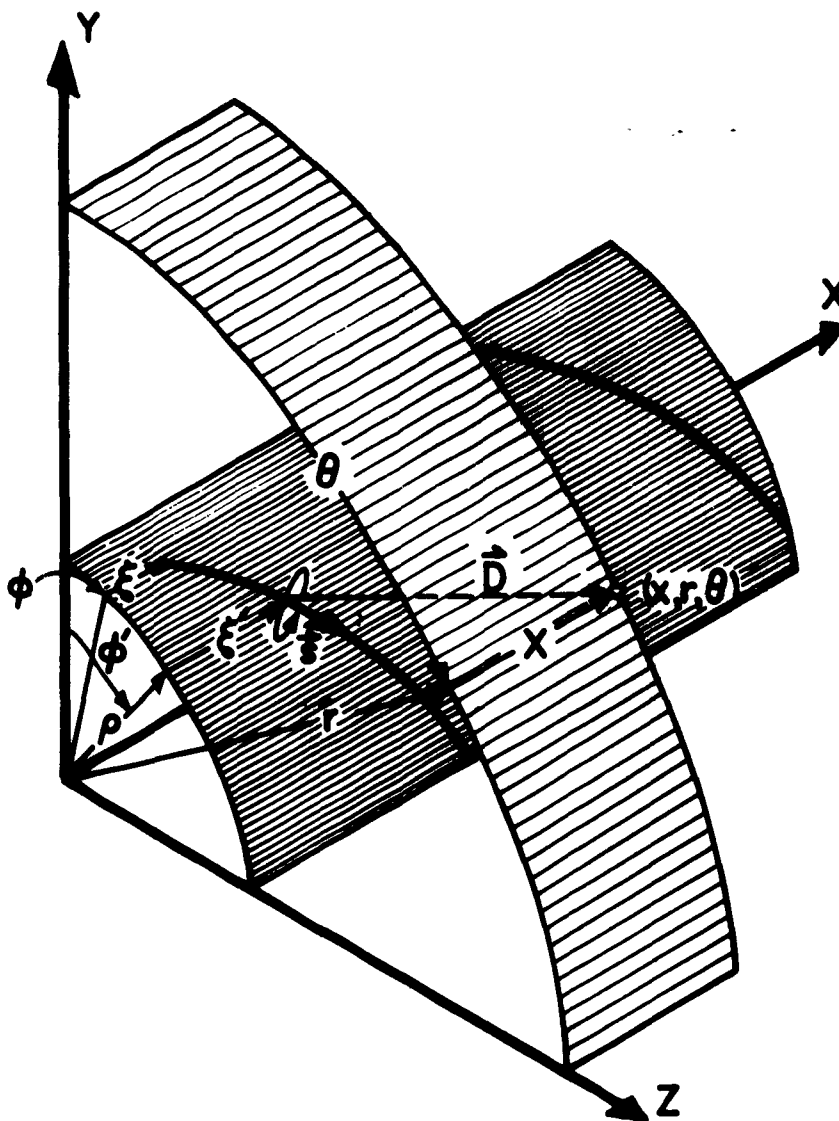$$\vec{s} = \frac{1}{\sqrt{\rho^2 + \lambda^2(\rho)}} \left[\lambda(\rho), \; -\rho\sin\varphi', \; \rho\cos\varphi' \right] \tag{6.3}$$

31

FIG. 6.1 NOTATION FOR VELOCITY AT
(x,r,φ) INDUCED BY AN ELEMENT
OF A TRAILER AT (ξ′,ρφ). THE
TRAILER ORIGINATES AT (ξ ,ρ,φ).

The three velocity components can be obtained by substituting (6.2) and (6.3) in (6.1)

$$\bar{u}(x,r,\theta,\xi,\rho,\phi) = \frac{1}{4\pi} \int_{\phi'=\phi}^{\infty} \frac{(\rho^2 - \rho r \cos(\phi' - \theta) \, d\phi'}{\left[(x - \xi')^2 + r^2 + \rho^2 - 2r\rho\cos\phi'\right]^{3/2}}$$

(6.4)

$$\bar{v}(x,r,\theta,\xi,\rho,\phi) = \frac{1}{4\pi} \int_{\phi'=\phi}^{\infty} \frac{\left[(x - \xi')\rho\cos\phi' - \lambda(\rho)r\sin\theta + \lambda(\rho)\rho\sin\phi'\right]d\phi'}{\left[(x - \xi')^2 + r^2 + \rho^2 - 2r\rho\cos\phi'\right]^{3/2}}$$

$$\bar{w}(x,r,\theta,\xi,\rho,\phi) = \frac{1}{4\pi} \int_{\phi'=\phi}^{\infty} \frac{\left[\lambda(\rho)r\cos\theta - \lambda(\rho)\rho\cos\phi' + (x - \xi')\rho\sin\phi'\right]d\phi'}{\left[(x - \xi')^2 + r^2 + \rho^2 - 2r\rho\cos\phi'\right]^{3/2}}$$

In these equations the variable of integration has been converted from s' to ϕ' using the relation

$$ds' = \sqrt{\rho^2 + \lambda^2(\rho)} \; d\phi'$$

(6.5)

The velocity components in (6.4) can be resolved into axial tangential and radial components as done before for the sources and bound vortices

$$\bar{u}_a = \bar{u} = \frac{1}{4\pi} \int_{\phi'=\phi}^{\infty} \frac{\left[\rho^2 - \rho r \cos(\phi' - \theta)\right]d\phi'}{\left[(x - \xi')^2 + r^2 + \rho^2 - 2r\rho\cos\phi'\right]^{3/2}}$$

33

$$\bar{u}_t = \bar{w}\cos\theta - \bar{v}\sin\theta = \frac{1}{4\pi}\int_{\varphi'=\varphi}^{\infty}\frac{\left[\lambda(\rho)\,(r - \rho\cos(\varphi'-\theta)) + (x-\zeta')\rho\,\sin(\varphi'-\theta)\right]d\varphi'}{\left[(x-\zeta')^2 + r^2 + \rho^2 - 2r\rho\cos\varphi'\right]^{3/2}}$$

$$(6.6)$$

$$\bar{u}_r = \bar{w}\sin\theta + \bar{v}\cos\theta = \frac{1}{4\pi}\int_{\varphi'=\varphi}^{\infty}\frac{\left[\lambda(\rho)\rho\,\sin(\varphi'-\theta) + (x-\zeta')\rho\,\cos(\varphi'-\theta)\right]d\varphi'}{\left[(x-\zeta')^2 + r^2 + \rho^2 - 2r\rho\cos\varphi'\right]^{3/2}}$$

The component normal to the helicoidal surface at (r, θ) is obtained by combining (6.6) and (3.5)

$$\bar{u}_n(x,r,\theta,\zeta,\rho,\varphi) = \frac{1}{4\pi\sqrt{r^2 + \lambda^2(r)}} \cdot \int_{\varphi'=\varphi}^{\infty}$$

$$\frac{r\rho^2 - r^2\rho\cos(\varphi'-\theta) - \lambda(r)\lambda(\rho)\{r-\rho\cos(\varphi'-\theta)\} - (x-\zeta')\rho\lambda(r)\sin(\varphi'-\theta)\ d\varphi'}{\left[(x-\zeta')^2 + r^2 + \rho^2 - 2r\rho\cos\varphi'\right]^{3/2}}$$

$$(6.7)$$

By again introducing the approximation

$$x - \zeta' = \lambda(r)\theta - \lambda(\rho)\varphi' \approx -\lambda(\rho)(\varphi'-\theta) = -\lambda(\rho)v$$

which is equivalent to (3.9) and (5.8) and replacing $\varphi'-\theta$ by $v + \delta_k$ (6.7) becomes

$$\bar{u}_n(r,\rho,\mu,k) = \frac{1}{4\pi\sqrt{r^2 + \lambda^2(r)}} \int_{v=\mu}^{\infty}$$

$$\frac{\left[(\lambda(r)\lambda(\rho)\rho - r^2\rho)\cos(v + \delta_k) + \lambda(r)\lambda(\rho)\rho v\,\sin(v + \delta_k) - r(\lambda(r)\lambda(\rho)-\rho^2)\right]dv}{\left[\lambda^2(\rho)v^2 + r^2 + \rho^2 - 2r\rho\cos(v + \delta_k)\right]^{3/2}}$$

$$(6.8)$$

The velocity induced by K unit trailers is obtained by summing (6.8) over the blades

$$T(r,\rho,\mu) \;=\; \sum_{k=1}^{K} \bar{u}_n(r,\rho,\mu,k) \tag{6.9}$$

The total velocity is obtained by introducing the strength of the trailers given in (4.5), (4.9) and (4.11) and integrating over the blade surface.

$$u_n^{(t)}(r,\theta) = - \oint_{r_h}^{1.0} \oint_{\theta_L(\rho)-\theta}^{\theta_T(\rho)-\theta} \frac{\partial}{\partial\rho}\left[\gamma(\rho,\,\mu+\theta)\sqrt{\rho^2+\lambda^2(\rho)}\right]T(r,\rho,\mu)d\mu\,d\rho +$$

$$\tag{6.10}$$

$$\oint_{r_h}^{1.0}\left[\gamma(\rho,\theta_L(\rho))\,T(r,\rho,\theta_L(\rho)-\theta)\frac{\partial\theta_L(\rho)}{\partial\rho} - \gamma(\rho,\theta_T(\rho))\,T(r,\rho,\theta_T(\rho)-\theta)\frac{\partial\theta_T(\rho)}{\partial\rho}\right]$$

$$\sqrt{\rho^2+\lambda^2(\rho)}\,d\rho$$

The first integral in (6.10) represents the contribution of the trailers originating from points in the interior of the blades, while the second integral takes into account the trailers starting at the leading and trailing edges. The Cauchy principal value of the integrals must be taken whenever the range of integration includes the point (r,θ) where the velocity is to be determined.

35

While the expressions for the velocity induced by the sources and bound vortices are not particularly simple, (6.10) is a much more difficult expression to evaluate due to the fact that the function $T(r,\rho,\mu)$ involves an integration over a semi-infinite interval. However, this difficulty can be eliminated by considering T as the sum of the two functions

$$T = T_o + T_1 \qquad (6.11)$$

obtained by splitting up the range of integration in (6.8) in such a way that

$$T_o(r,\rho) = T(r,\rho,o) = \frac{1}{4\pi\sqrt{r^2 + \lambda^2(r)}} \int_o^\infty f(v)\,dv \qquad (6.12)$$

and

$$T_1(r,\rho,\mu) = \frac{-1}{4\pi\sqrt{r^2 + \lambda^2(r)}} \int_o^\mu f(v)\,dv \qquad (6.13)$$

where $f(v)$ is the integrand of (6.8).

It is evident that $f(v)$ is an even function if one applies the same argument used in sections 3 and 5. Consequently,

$$T_o(r,\rho) = \frac{1}{8\pi\sqrt{r^2 + \lambda^2(r)}} \int_{-\infty}^\infty f(v)\,dv \qquad (6.14)$$

is one-half of the velocity induced by a set of K unit helicoidal vortices extending from $(-\infty,\infty)$. Since the velocity field of such a configuration is two dimensional (it is independent of s in the (s,n,r) coordinate system) an alternate expression for T_o can be obtained from a two

36

dimensional potential. A derivation of this potential was given by Lerbs[9] who found the result to be an infinite series of modified Bessel Functions[*]. While this, in itself, would offer no particular computational advantage over the integral representation given in (6.13), it is fortunate that highly accurate asymptotic approximations to the sums of Bessel functions are available. The most accurate approximations were developed by Wrench[10], and it has been found that his formulas are far more efficient than the numerical integration required to evaluate (6.13). The exact and approximate expressions for T_o, taken from Lerbs' and Wrench's work with some modification in nomenclature, appear in Appendix A.

We consider finally the second part of (6.10), namely T_1. Since $f(v)$ is even, T_1 is an odd function of μ

$$T_1(r,\rho,-\mu) = -T_1(r,\rho,\mu) \tag{6.15}$$

This fact is not only useful in the numerical evaluation of T_1, but also permits us to draw some important conclusions regarding incidence and camber which will be considered in the next section.

---

[*]Lerbs' results are expressed in terms of "induction factors" which differ from T_o by a constant factor.

7. Total Disturbance Velocity Normal to the Blades

The total disturbance velocity normal to the first blade at a point (r,θ) is obtained by summing the effects of thickness (3.17), bound vortices (5.10) and trailers (6.10)

$$u_n(r,\theta) = u_n^{(s)}(r,\theta) + u_n^{(b)}(r,\theta) + u_n^{(t)}(r,\theta) \qquad (7.1)$$

We can further subdivide $u_n^{(t)}$ into parts, $u_n^{(t_0)}$ and $u_n^{(t_1)}$, where the former represents the contribution of T_0 and the latter the contribution of T_1 as defined in (6.12) and (6.13). An expression for $u_n^{(t_0)}$ can be obtained from (6.10) be replacing $T(r,\rho,\mu)$ by $T_0(r,\rho)$ and bringing T_0 outside the μ integration (since it is independent of μ)

$$u_n^{(t_0)}(r) = \int_{\rho=r_h}^{1.0} T_0(r,\rho) \left\{ - \int_{\mu=\theta_L(\rho)-\theta}^{\theta_T(\rho)-\theta} \frac{\partial}{\partial\rho}\left[\gamma(\rho,\varphi+\theta)\sqrt{\rho^2+\lambda^2(\rho)}\right]d\mu \; + \right.$$

$$\qquad (7.2)$$

$$\left[\gamma(\theta_L(\rho)\rho)\frac{\partial\theta_L(\rho)}{\partial\rho} - \gamma(\theta_T(\rho)\,\rho)\frac{\partial\theta_T(\rho)}{\partial\rho}\right]\sqrt{\rho^2+\lambda^2(\rho)} \left. \right\} d\rho$$

This can be simplified using (4.13) and (4.14) to

$$u_n^{(t_0)}(r) = - \int_{\rho=r_h}^{1.0} \frac{\partial\Gamma(\rho)}{\partial\rho} \, T_0(r,\rho)\,d\rho \qquad (7.3)$$

where $\Gamma(\rho)$, as defined in (4.3), is the total circulation around each blade at a radius ρ. This is well-known as the "lifting-line" equation which represents the velocity induced by the trailers shed from K concentrated radial bound vortices.

38

The lifting-line approximation to $u_n(r)$ is obtained by determining $u_n^{(t_0)}$ from (7.3) and approximating $u_n^{(b)}(r,\theta)$ from two-dimensional theory based on the sections at the particular radius in question. The latter approximation is frequently referred to as "strip theory." The velocity components $u_n^{(s)}$ and $u_n^{(t_1)}$ are assumed to be zero in lifting-line theory. However, these assumptions are valid only when the aspect ratio of the blades is large, which is never true in the case of a marine propeller. Consequently, the lifting-line velocity $u_n^{(t_0)}(r)$ is of limited usefulness in itself and should therefore be considered simply as one of the ingredients in the total velocity given in (7.1).

We see from (7.3) that $u_n^{(t_0)}(r)$ represents a disturbance velocity which is constant over the chord. The remaining terms in (7.1) are generally functions of both r and θ and depend on the blade outline and the load and thickness distribution.

We now consider the special case where the blade outline, chordwise load distribution and chordwise thickness distribution is symmetrical about the lines $\theta = \delta_k$ through the tips of the blades. In this case, it can be shown that $u_n^{(s)}(r,\theta)$ is an even function of θ, while $u_n^{(b)}(r,\theta)$ and $u_n^{(t_1)}(r,\theta)$ are odd functions of θ.

Consider first the velocity due to the sources, $u_n^{(s)}(r,\theta)$. It was shown in section 3 that the function $S(r,\rho,\mu)$ is an odd function of μ. Recalling that $\mu = \varphi - \theta$, we can write

$$S(r,\rho,\varphi - \theta) = -S(r,\rho, -\varphi + \theta) \tag{7.4}$$

Since the blade outline is symmetrical, we also know that

$$\theta_L(\rho) = -\theta_T(\rho) \tag{7.5}$$

39

while the fact that the thickness form is symmetrical about the mid-chord requires that the source strength be an odd function of φ

$$\sigma(\rho,\varphi) = -\sigma(\rho-\varphi) \tag{7.6}$$

The total velocity induced at a point (r,θ) by the sources according to (3.12) is

$$u_n^{(s)}(r,\theta) = \int_{r_h}^{1.0} \sqrt{\rho^2 + \lambda^2(\rho)} \int_{\theta_L(\rho)}^{\theta_T(\rho)} \sigma(\rho,\varphi)\, S(r,\rho,\varphi-\theta)\, d\varphi\, d\rho \tag{7.7}$$

while the velocity induced at the corresponding point $-\theta$ is

$$u_n^{(s)}(r,-\theta) = \int_{r_h}^{1.0} \sqrt{\rho^2 + \lambda^2(\rho)} \int_{\theta_L(\rho)}^{\theta_T(\rho)} \sigma(\rho,\varphi)\, S(r,\rho,\varphi+\theta)\, d\varphi\, d\rho \tag{7.8}$$

We next introduce the symmetry properties expressed in (7.4), (7.5) and (7.6) in (7.8) to obtain

$$u_n^{(s)}(r,-\theta) = \int_{r_h}^{1.0} \sqrt{\rho^2 + \lambda^2(\rho)} \int_{-\theta_T(\rho)}^{-\theta_L(\rho)} \sigma(\rho,-\varphi)\, S(r,\rho,-\varphi-\theta)\, d\varphi\, d\rho \tag{7.9}$$

Substituting $-\varphi$ for φ as the variable of integration in (7.9) and changing the sign of the limits of integration accordingly, we obtain

$$u_n^{(s)}(r,-\theta) = -\int_{r_h}^{1.0} \sqrt{\rho^2 + \lambda^2(\rho)} \int_{\theta_T(\rho)}^{\theta_L(\rho)} \sigma(\rho,\varphi)\, S(r,\rho,\varphi-\theta)\, d\varphi\, d\rho \tag{7.10}$$

Since this is the negative of (7.7) except with the upper and lower limits of integration reversed, we conclude finally

$$u_n^{(s)}(r,\theta) = u_n^{(s)}(r,-\theta) \qquad (7.11)$$

The velocities $u_n^{(b)}(r,\theta)$ and $u_n^{(t_1)}(r,\theta)$ can be shown to be odd functions of θ in exactly the same way. In this case $B(r,\rho,\mu)$ and $T(r,\rho,\mu)$ are odd functions of μ as was $S(r,\rho,\mu)$ while the strength of the bound vortices and trailers is an even function of φ. This introduces an additional minus sign in going from the equivalent of (7.8) and (7.9). Consequently, we conclude that

$$u_n^{(b)}(r,\theta) = -u_n^{(b)}(r,-\theta)$$

$$u_n^{(t_1)}(r,\theta) = -u_n^{(t_1)}(r,-\theta)$$

$$(7.12)$$

An important conclusion which can be drawn from (7.12) is that a propeller of zero thickness with symmetrical blades and load distribution will require no additional incidence beyond that given by lifting-line theory, i.e., the contribution of $u_n^{(t_0)}(r)$. An additional incidence correction (aside from corrections due to viscosity) can appear only as a result of blade thickness. The lifting surface correction therefore consists entirely of camber in this case. Conversely, the thickness distribution cannot induce a net camber since it is an even function of θ.

These conclusions obviously do not hold if the assumed symmetry is not present.

41

8. Non-Linear Refinements

According to linear theory, the singularities representing pressure loading and thickness are distributed on stream surfaces formed by the undisturbed approach flow. Some improvement in accuracy would presumably be achieved if the sources and vortices on the blades were located on the mean lines of the sections at each radius and if the trailers were made to follow the actual streamlines extending downstream from the trailing edges of the blades. However, in this case the position of the singularities would depend on the disturbance velocity field which, in turn, would depend on the position of the singularities.

While a complete solution of this non-linear problem is presently considered to be both impractical and unnecessary, there is one refinement which may be introduced with very little additional complication. This is customarily referred to as the theory of "moderately loaded" propellers, as contrasted to the strictly linearized case which is termed "lightly loaded."

In the moderately loaded case, it is still assumed that the distortion of the oncoming flow due to the radial component of the disturbance velocity is negligible. Consequently, the streamlines remain on cylindrical surfaces as before. However, in this case, the distortion of the streamlines due to the axial and tangential disturbance velocities is taken into account in an approximate way. It is assumed that the resultant streamlines lie on helicoidal surfaces whose pitch includes the lifting line disturbance velocities obtained from (7.3). The modified surface can be expressed in terms of a hydrodynamic pitch angle β_i, which can be seen from Figure 8.1 to be:

$$\tan \beta_i(r) = \frac{u_a^{(t_0)}(r) + V_A(r)}{\omega r + u_t^{(t_0)}(r)} \tag{8.1}$$

It should be noted that the tangential disturbance velocity is negative in Figure 8.1, which is evident if one compares Figure 8.1 with the velocity diagram shown in Figure 2.3. The plus sign in the denominator of 8.1 is therefore consistent with this sign convention.

A hydrodynamic advance coefficient λ_i can be defined as

$$\lambda_i(r) = r \tan\beta_i(r) \tag{8.2}$$

which is analogous to the definition of λ in (2.4). Finally the resultant approach velocity V^* can be seen from Figure 8.1 to be:

$$V^*(r) = \frac{V_A(r) + u_a^{(t_0)}(r)}{\sin\beta_i(r)} = \frac{\omega r + u_t^{(t_0)}(r)}{\cos\beta_i(r)} \tag{8.3}$$

The lifting line disturbance velocities for a prescribed radial load distribution may be obtained from (7.3) as before. The only difference is that λ is replaced by λ_i in the expression for T_0. As a result, T_0 becomes a function of $u_a^{(t_0)}$ through λ_i so that (7.3) represents a non-linear integral equation rather than simply an integral. However, a solution can readily be obtained by an iterative scheme where the j'th approximation to u_n is obtained by using the value λ_i obtained in the (j - 1)st iteration in determining T_0. The first approximation is simply the linear one, i.e., $\lambda_i = \lambda$.
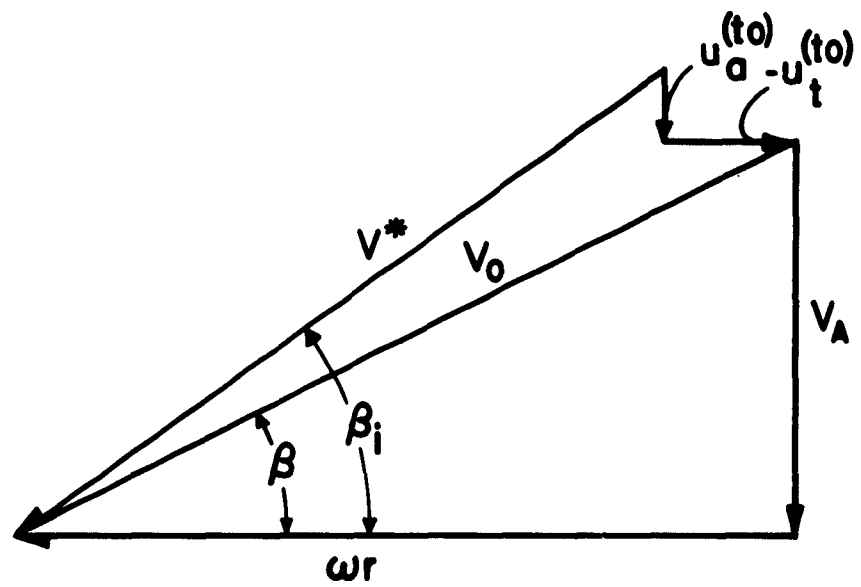
43

FIG. 8.1   VELOCITY DIAGRAM AT A
LIFTING LINE

Once λ_1 is determined, the evaluation of the remaining velocity components $u_a^{(s)}$, $u_n^{(b)}$ and $u_n^{(t_1)}$ can be accomplished in the same way as in the completely linearized case. Consequently, the only additional complication introduced in the theory of moderately loaded propellers is that an iterative solution is required to solve the lifting line equation.

References

1. Sparenberg, J. A., "Application of Lifting Surface Theory to Ship Screws," Proceedings of the Koninkl. Nederl. Akademie van Wetenschappen, Amsterdam Series B, 62, No. 5, 1959.

2. Pien, P. C., "The Calculation of Marine Propellers Based on Lifting Surface Theory," Journal of Ship Research, Vol. 5, No. 2, September, 1961.

3. van Manen, J. D. and Bakker, A. R., "Numerical Results of Sparenberg's Lifting Surface Theory for Ship Screws," Fourth Symposium on Naval Hydrodynamics, Washington, D. C. August, 1962.

4. Kerwin, J. E., "The Solution of Propeller Lifting Surface Problems by Vortex Lattice Methods," Department of Naval Architecture and Marine Engineering, Massachusetts Institute of Technology, June, 1961.

5. Kerwin, J. E. and Leopold, R., "Propeller Incidence Correction Due to Blade Thickness," M. I. T., May, 1963 (to be published).

6. English, J. W., "The Application of a Simplified Lifting Surface Technique to the Design of Marine Propellers," National Physical Laboratory, SH R. 30/62, July, 1962.

7. Cox, G. G., "Corrections to the Camber of Constant Pitch Propellers," Quarterly Trans. of the Royal Institute of Naval Architecture, January, 1961.

8. Bisplinghoff, R. L., Ashley, H. and Halfman, R. L., "Aeroelasticity," Addison-Wesley Publishing Company, Inc., Mass., 1957.

9. Lerbs, H. W., "Moderately Loaded Propellers with Finite Number of Blades and an Arbitrary Distribution of Circulation," SNAME, 1952.

10. Wrench, J. W., Jr., "The Calculation of Propeller Induction Factors," DTMB Report 1116, February, 1957

APPENDIX

Summary of Expressions for Induced Velocities at a Lifting Line

The axial and tangential velocity induced by K helicoidal vortex lines of unit strength is given in (6.6). The lifting-line case is obtained by setting $\theta = \varphi = x = 0$ and by replacing φ' by $v + \delta_k$ and ζ' by $\lambda(\rho)v$

$$\bar{u}_a(r,\rho) = \frac{1}{4\pi} \int_0^\infty \frac{\{\rho^2 - \rho r \cos(v + \delta_k)\}\, dv}{\left[\lambda^2(\rho)v^2 + r^2 + \rho^2 - 2r\rho\cos(v + \delta_k)\right]^{3/2}}$$

$$\bar{u}_t(r,\rho) = \frac{1}{4\pi} \int_0^\infty \frac{\{\lambda(\rho)(r - \rho\cos(v + \delta_k)) - \lambda(\rho)v\rho\, \sin(v + \delta_k)\}\, dv}{\left[\lambda^2(\rho)v^2 + r^2 + \rho^2 - 2r\rho\, \cos(v + \delta_k)\right]^{3/2}}$$

(A-1)

Equivalent expressions are given by Lerbs[9] in terms of modified Bessel functions. With some slight changes in nomenclature and sign conventions, these results are

for $r < \rho$

$$\bar{u}_a(r,\rho) = \frac{K}{4\pi\, \lambda(\rho)} \left[1 - \frac{2K\rho F_1}{\lambda(\rho)} \right]$$

$$\bar{u}_t(r,\rho) = \frac{K^2 \rho\, F_1}{2\pi r\, \lambda(\rho)}$$

where

$$F_1 = \sum_{n=1}^\infty n\, I_{nK}\left\{\frac{nKr}{\lambda(\rho)}\right\} K'_{nK}\left\{\frac{nK\rho}{\lambda(\rho)}\right\}$$

(A.2)

47

and where $\mathbf{I}$ and $\mathbf{K}$ are the modified Bessel functions of the first and second kind respectively, and the prime denotes differentiation with respect to the arguments.

For $r > \rho$

$$\bar{u}_a(r,\rho) = \frac{-K^2 \rho F_2}{2\pi \, \lambda^2(\rho)}$$

$$\bar{u}_t(r,\rho) = \frac{K}{4\pi r}\left[1 + \frac{2K\rho F_2}{\lambda(\rho)}\right] \tag{A.3}$$

$$F_2 = \sum_{n=1}^{\infty} n \, K_{nK}\left\{\frac{nKr}{\lambda(\rho)}\right\} I'_{nK}\left\{\frac{nK\rho}{\lambda(\rho)}\right\}$$

The approximations to F_1 and F_2 developed by Wrench[10] are

$$F_1 \approx \frac{-1}{2Kq_0}\left(\frac{1+q_0^2}{1+q^2}\right)^{1/4}\left\{\frac{1}{U^{-1}-1} + \frac{1}{24K}\left[\frac{9q_0^2+2}{(1+q_0^2)^{3/2}} + \frac{3q^2-2}{(1+q^2)^{3/2}}\right]\log\left(1+\frac{1}{U^{-1}-1}\right)\right\}$$

$$F_2 \approx \frac{1}{2Kq_0}\left(\frac{1+q_0^2}{1+q^2}\right)^{1/4}\left\{\frac{1}{U-1} - \frac{1}{24K}\left[\frac{9q_0^2+2}{(1+q_0^2)^{3/2}} + \frac{3q^2-2}{(1+q^2)^{3/2}}\right]\log\left(1+\frac{1}{U-1}\right)\right\}$$

where $\quad q_0 = \rho/\lambda(\rho) \qquad q = r/\lambda(\rho)$ \hfill (A.4)

$$U = \left\{\frac{q_0(\sqrt{1+q^2}-1)}{q(\sqrt{1+q_0^2}-1)} \; \exp\left[\sqrt{1+q^2} - \sqrt{1+q_0^2}\right]\right\}^K$$

The quantities $\bar{u}_a(r,\rho)$ and $\bar{u}_t(r,\rho)$ can be converted to "induction factors" as follows:

$$i_a(r,\rho) = - 4\pi(r-\rho) \; \bar{u}_a(r,\rho) \tag{A.5}$$

$$i_t(r,\rho) = 4\pi(r-\rho) \; \bar{u}_t(r,\rho)$$

When defined in this way, the induction factors are always positive for a right-handed helix. The minus sign in the expression for $i_a(r,\rho)$ is not present in Equation 6 of Reference (9) where induction factors are first defined, but it is incorporated in later expressions in the paper.

The reason for defining an induction factor is to obtain a quantity which approaches a finite limit as $r \to \rho$. These limits, as derived by Lerbs and others, are

$$i_a(r,\rho) \to \cos\beta(\rho)$$

$$\tag{A.6}$$

$$i_t(r,\rho) \to \sin\beta(\rho)$$

Finally, the quantity $T_o(r,\rho)$, which represents the velocity normal to the helicoidal surface at a point r on the lifting line can be expressed in terms of induction factors using (3.5) and (A.5)

$$T_o(r,\rho) = \frac{r\bar{u}_a(r,\rho) - \lambda(r) \, \bar{u}_t(r,\rho)}{\sqrt{r^2 + \lambda^2(r)}} = \frac{ri_a(r,\rho) + \lambda(r) \, i_t(r,\rho)}{4\pi(\rho - r)\sqrt{r^2 + \lambda^2(r)}} \tag{A.7}$$

Copies

Copies		Copies	
75	Commanding Officer and Director David Taylor Model Basin Washington 7, D. C. ATTN: Code 513	1	Chief Bureau of Weapons Dept. of the Navy Washington 25, D. C.

10 Chief
    Bureau of Ships
    Department of the Navy
    Washington 25, D. C.
    ATTN:
 3 Techn. Information Bu. (Code 335)
 1 Ship Design (Code 410)
 1 Ship Silencing Branch (Code 345)
 1 Preliminary Design (Code 420)
 1 Hull Design (Code 440)
 1 Scientific and Research (Code 442)
 1 Hull, Arrgts, & Seamanship (Code 341B)

 2 Director
    Ordance Research Lab.
    Pennsylvania State University
    P. O. Box 30
    University Park, Pa.

 1 Mr. Hollinshead De Luce
    Bethlehem Steel Co.
    Shipbuilding Division
    Quincy 69, Massachusetts

 2 Gibbs and Cox, Inc.
    21 West Street
    New York 6, New York
    ATTN: Mr. W. F. Gibbs
           Mr. W. Bachman

 1 Reed Research Inc.
    1048 Potomac Street, N. W.
    Washington 7, D. C.
    ATTN: Mr. S. Reed

 2 Dr. A. G. Strandhagen, Head
    Department of Engineering Mechanics
    University of Notre Dame
    Notre Dame, Indiana

 1 Dr. J. V. Wehausen
    Department of Engineering
    Inst. of Engineering Research
    University of California
    Berkeley 4, California

 1 Chief
    Bureau of Weapons
    Dept. of the Navy
    Washington 25, D. C.

 2 Commander
    U. S. Naval Ord. Lab.
    White Oak
    Silver Spring, Md.
    ATTN: Library

 1 Commanding Officer
    ONR
    Branch Office
    495 Summer Street
    Boston 10, Mass.

 1 Commanding Officer
    ONR
    Branch Office
    John Crerar Library Bldg.
    10th Floor
    86 E. Randolph Street
    Chicago 1, Illinois

 1 Commanding Officer
    ONR
    Branch Office
    1031 E. Green Street
    Pasadena 1, Calif.

 1 Director
    Hydrodynamics Lab.
    California Inst. of Tech.
    Pasadena 4, Calif.

 1 Prof. J. A. Schade
    Inst. of Eng. Research
    University of Calif.
    Berkeley 4, California

 1 Editor
    Engineering Index, Inc.
    29 West 39th Street
    New York, New York

 1 Librarian
    Inst. of Aero. Sciences
    2 E. 64th Street
    New York 21, New York

Copies

Copies		Copies	
2	Electric Boat Division General Dynamics Corp. Groton, Connecticut ATTN: Mr. H. E. Sheets Mr. R. J. McGrattan	2	Technical Research Group, Inc. 2 Aerial Way Syosset, New York ATTN: Dr. J. Kotik Dr. J. Lurye
2	General Applied Science Lab. Merrick and Stewart Avenues Westbury, Long Island, New York ATTN: Dr. Simon Slutsky Mr. E. Lieberman	1	Vidya 1450 Page Mill Road Palo Alto, California ATTN: Dr. A. H. Sacks
2	Grumman Aircraft Eng. Corp. Bethpage Long Island, New York ATTN: Dr. S. Ciolkowski Mr. C. Squires	2	Therm, Incorporated Therm Advanced Research Ithaca, New York ATTN: Dr. A. Ritter Dr. S. C. Ling
2	Hydronautics, Inc. Pindell School Road Howard County Laurel, Maryland ATTN: Mr. P. Eisenberg Mr. M. P. Tulin	15	Stevens Institute of Tech. Davidson Laboratory Castle Point Station Hoboken, New Jersey
2	Iowa Institute of Hydraulic Res. University of Iowa Iowa City, Iowa ATTN: Dr. Hunter Rouse Prof. L. Landweber	3 1 1 1 1	ATTN: Dr. J. P. Breslin Mr. Paul Spens Mr. P. A. Lalangas Dr. Pung Hu Dr. S. Tsakonas Miss W. Jacobs Mr. C. J. Henry Mr. M. Raihan Mr. A. Strumpf Dr. S. Lukasik Mr. D. Savitsky Mr. E. Numata Mr. T. Kowalski
2	University of Michigan Dept. of Naval Arch. and Marine Engineering Ann Arbor, Michigan ATTN: Dr. F. C. Michelsen Prof. R. B. Couch		
7	University of Minnesota St. Anthony Falls Hydraulic Lab. Minneapolis 14, Minnesota ATTN: Dr. L. G. Straub Prof. E. Silberman Prof. John Ripken Mr. J. Killen Prof. C. E. Bowers Prof. C. S. Song Mr. J. M. Wetzel		